Modeling Actomyosin Clustering depending on Medium ATP-Concentrations ⋆

Christian Wölfer * **Robert J. Flassig** * **Michael Mangold** *,**

* *Max Planck Institute for Dynamics of Complex Technical Systems, 39106 Magdeburg, Germany*
** *TH Bingen, 55411 Bingen am Rhein, Germany*

Keywords: Actin-Myosin Cortex, Dynamic Modeling, Distributed Model, System Analysis, Synthetic Biology

1. INTRODUCTION

The cell cortex, formed by membrane linked actin filaments, is an important functional unit of almost all eukaryotic cells and involved in a variety of major cellular processes like cell division, motility, formation and stabilization of cell shape(Alberts et al., 1994). Hence, modeling and understanding of the cell cortex is of great interest in the context of bottom-up synthetic biology (Schwille, 2011).
The polymeric and filamentous protein F-actin forms the mesh-like and therefore viscoelastic material. Together with the myofilament myosin II, a filamentous protein with a variety of motor domain (Fig. 1b), the cortex has active gel properties.
An experimental study with a synthetic 'minimal actin cortices' (Vogel and Schwille, 2012) showed that spatial cluster formation of actin cortices only occur in a range of 0.1 to 10 μM and surprisingly not for high ATP concentrations (Vogel et al., 2013).

2. THE ACTOMYOSIN MODEL

To explain the experimental findings qualitatively a two dimensional continuum model was developed in polar coordinates to represent a cut through a spherical cell or vesicle. Additionally, the actomyosin cortex properties were mimicked by assuming that the actin and myosin species remain close to the membrane in a very thin layer. Thus, the actomyosin cortex can be described as a one dimensional ring system with periodic boundary conditions. In contrast, the energy source ATP, which is consumed by the cortex, diffuses from the inside through the whole two dimensional system (A.1). The spatial distribution of the cortex species obeys an advection-diffusion equation with additional mass action reaction rates (A.2-A.4).
The underlying force generating biochemical circuit is the well described myosin cross bridge cycle (Rayment et al., 1993). We used a simplified spatial distributed myosin cross bridge model (Fig. 1a) where energy provided by ATP hydroxylation causes a conformational change of the myosin head (M). The active myosin head is able to interact with F-actin forming an active actomyosin complex (A-M). The unstable active actomyosin complex performs a further conformational change of the myosin head triggering an acceleration of the F-actin filament due to the mechanical coupling. To close the cycle, ATP is needed to release the myosin head from the F-actin filament.
We assumed that the binding and releasing of the myosin head are the rate-determining steps. Thus, force generation and the ATP hydroxylation take place during myosin binding (r_1) and detachment (r_2).
The momentum equation with viscoelastic material behaviors is described by

$$\frac{D(\rho \boldsymbol{v})}{Dt} = \frac{\partial}{\partial \varphi}(\sigma_v + \sigma_e + \sigma_m), \tag{1}$$

consisting of the material derivation for F-actin momentum $\rho \boldsymbol{v}$, and terms for viscous stress σ_V as one dimensional representation of the viscous stress tensor $\tau_{\varphi\varphi}$ (Bird et al., 1960), elastic stress $\sigma_e = \alpha A^2(1-e)$ derived by Lewis et al. (2014) with the related evolution of network deformation e (A.5) and the contractile stress σ_m generated by the myosin pulls.
As a new approach, the contractile stress is modeled by the force generating mass action rate r_1 times a force transmission state χ:

$$\sigma_m = \psi \cdot r_1 \cdot \chi \tag{2}$$

The fundamental idea is that the myosin can only bend, break or compact filaments when on both sides of the myofilament (Fig. 1b) enough heads are connected to the F-actin mesh (Wölfer et al., 2016). Otherwise, the power stroke would not be transmitted sufficiently and instead move the myosin molecule along the actin filament. The force transmission should increase the more myosin heads are bound to the actin filament. Thus, in our formulation the local force transmission is determined by the concentration of inactive actomyosin scaled by the total amount of myosin.

$$\chi = \frac{A\text{-}M}{A\text{-}M + M} \tag{3}$$

In contrast to other actin models (Jülicher et al., 2007; Ramaswamy and Jülicher, 2016) polymerization, depolymerization and, as a consequence, polarity of F-actin filaments were not taken into account because of an insignificant role of those processes in the underlying *in vitro* experiment Vogel et al. (2013).

⋆ This work is a part of the MaxSynBio consortium, which is funded by the German Federal Ministry of Education and Research and the Max Planck Society.

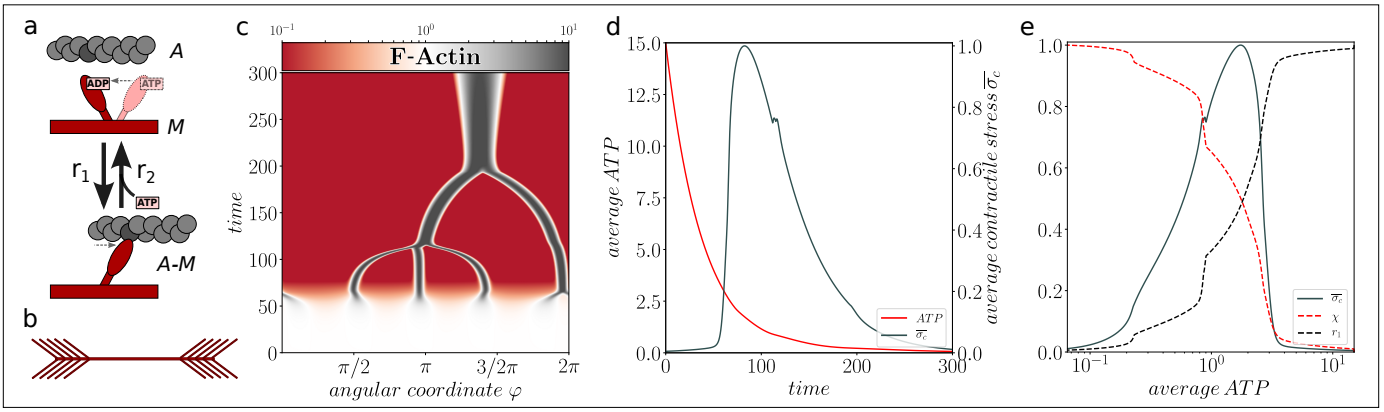

Fig. 1. a: Myosin cross bridge model b: myofilament c: clustering actin cortex d: average ATP concentration and normalized contractile stress over time e: normalized curves force generation r_1, transmission χ and contractile stress against average ATP conc.

3. RESULTS AND DISCUSSION

Simulation of the nondimensionalized and discretizised model showed that clustering occurs even when the ATP concentration (consumed in r_2) drops under 5 units according with an increase of the contractile stress σ_m (Fig. 1c,d). The network clustered gradually by merging of smaller clusters, pursuant to the periodic initial conditions, consistent to the experimental observations. Finally, the contraction ceases after ATP depletion, recognizable by diminishing of the cluster due to diffusion.

As expected, for high ATP level concentrations the generated force by r_1 is very high . Thus, the majority of myosin heads are in the unbound state resulting in a poor transmission of force χ and therefore small contractile stress σ_m or rather a movement of the myofilament along the actin fiber. With decreasing ATP concentration the force transmission is improved accompanied by a decreasing force generation, resulting in a nearly bell-shaped dose-response curve for σ_m (Fig. 1e).

Accordingly, we are able to generate the desired dose-response relation for ATP and resulting contraction, with the suggested formulation for contractile stress. In addition *in vitro* studies, which observed a movement of myosin proteins along actin filaments, support our new formulation (Sheetz and Spudich, 1983; Vogel et al., 2013).

REFERENCES

Alberts, B., Bray, D., Lewis, J., Raff, M., Roberts, K., and Watson, J.D. (1994). Molecular biology of the cell. 3rd. *New York: Garland Pub*, 43(1294), 67.

Bird, R.B., Stewart, W.E., and Lightfoot, E.N. (1960). *Transport Phenomena*. John Wiley and Sons.

Jülicher, F., Kruse, K., Prost, J., and Joanny, J.F. (2007). Active behavior of the cytoskeleton. *Physics Reports*, 449, 3–28.

Lewis, O.L., Guy, R.G., and Allard, J.F. (2014). Actin-myosin spatial patterns from a simplified isotropic viscoelastic model. *Biophysical journal*, 107, 863–870.

Ramaswamy, R. and Jülicher, F. (2016). Activity induces traveling waves, vortices and spatiotemporal chaos in a model actomyosin layer. *Scientific Reports 6*.

Rayment, I., Holden, H.M., Whittaker, M., Yohn, C.B., Lorenz, M., Holmes, K.C., and Milligan, R.A. (1993). Structure of the actin-myosin complex and its implications for muscle contraction. *Science*, 261, 58–65.

Schwille, P. (2011). Bottom-up synthetic biology: Engineering in a tinkerers world. *Science*, 333, 1252–1254.

Sheetz, M.P. and Spudich, J.A. (1983). Movement of myosin-coated fluorescent beads on actin cables in vitro. *Nature*, 303, 31–35.

Vogel, S.K., Petrasek, Z., Heinemann, F., and Schwille, P. (2013). Myosin motors fragment and compact membrane-bound actin filaments. *Cytoskeleton (Hoboken)*, 70, 706–717.

Vogel, S.K. and Schwille, P. (2012). Minimal systems to study membrane-cytoskeleton interactions. *Curr Opin Biotechnology*, 23, 758–765.

Wölfer, C., Vogel, S.K., and Mangold, M. (2016). A curvilinear model approach: Actin cortex clustering due to atp-induced myosin pulls. *IFAC-PapersOnLine*, 49(26), 103–108.

Appendix A. PDE SYSTEM

$$\frac{\partial ATP}{\partial t} = D_T \left(\frac{1}{R}\frac{\partial}{\partial R}\left(R\frac{\partial ATP}{\partial R}\right) + \frac{1}{R^2}\frac{\partial^2 ATP}{\partial \varphi^2}\right) \quad \text{(A.1)}$$

$$\frac{\partial A}{\partial t} = -\frac{\partial (A\cdot V)}{\partial \varphi} + D_A \frac{\partial^2 A}{\partial \varphi^2} - r_1 + r_2 \quad \text{(A.2)}$$

$$\frac{\partial M}{\partial t} = -\frac{\partial (M\cdot V)}{\partial \varphi} + D_M \frac{\partial^2 M}{\partial \varphi^2} - r_1 + r_2 \quad \text{(A.3)}$$

$$\frac{\partial A\text{-}M}{\partial t} = -\frac{\partial (A\text{-}M\cdot V)}{\partial \varphi} + D_A \frac{\partial^2 A\text{-}M}{\partial \varphi^2} + r_1 - r_2 \quad \text{(A.4)}$$

$$\frac{\partial e}{\partial t} = -\frac{\partial (e\cdot V)}{\partial \varphi} + \lambda(1-e) \quad \text{(A.5)}$$